High-pressure synthesis of corundum-type $Ga_2O_3:Cr^{3+}$ and application of its fluorescence to the pressure scale

Hitoshi Yusa and Masashi Miyakawa*

Research Center for Materials Nanoarchitectonics, National Institute for Materials Science, 1-1 Namiki (NIMS), Tsukuba, Ibaraki 305-0044, Japan.

KEYWORDS (gallium oxides, corundum, doping, fluorescence, pressure scale).

ABSTRACT

Cr^{3+}-doped Ga_2O_3 crystals with a corundum structure were synthesized under high temperature and high pressure, and their excitation as well as fluorescence properties were evaluated. The crystals were green under white light illumination but deep red when exposed to ultraviolet light. This is mainly attributable to R_1 and R_2 fluorescence spectra caused by the Cr^{3+} transition. The pressure-dependence of their fluorescence spectra is comparable with ruby ($Al_2O_3:Cr^{3+}$), which is currently often used as a pressure scale. The excitation spectrum was shifted to the long-wavelength side compared with ruby, which enables excitation with long-wavelength lasers, even

if the pressure effect is considered. In addition, the R_1 and R_2 peaks were well-separated with increasing pressure, which might have advantages over the ruby scale.

Introduction

In recent years, gallium oxides (Ga_2O_3) have attracted attention in various fields for applications to power semiconductors and optics[1, 2]. However, such studies are mainly concerned with a monoclinic β phase (space group: *C*2/*m*), which is the stable phase at ambient pressure. The luminescence properties of Ga_2O_3 have also been studied for the β phase. The β phase consists of coordination numbers (CNs) 4 and 6. Other than the β phase, under high pressure, there are various polymorphs; such as corundum (CN 6), Rh_2O_3 (II) (CN 6), and $CaIrO_3$-type (CN 6 and 6+2) structures in Ga_2O_3[3, 4]. The corundum-type structure, which is the lowest high-pressure phase among them, can be recovered at ambient pressure. Thus, unlike other structures, there are reports in the 1960s [5, 6]. In accordance with ab initio calculations, small enthalpy of difference between the β and corundum phase implies high stability under ambient pressure [3]. The high stability is a crucial factor in its application as an optical material.

Ruby ($Al_2O_3:Cr^{3+}$) fluorescence is a typical example of chromium-doping of the corundum structure. Needless to say, the fluorescence properties played a leading role in the early days of laser research. Another aspect of ruby applications is the ruby fluorescence method to measure pressure in the field of high-pressure research[7]. This pressure scale is widely used for in-situ pressure measurement in a diamond anvil cell (DAC) [8-10], based on the pressure dependence of the ruby fluorescence peak (R_1 and R_2) originating from ligand-field splitting of Cr^{3+}. Since this method was first established in 1976 [8], it has been revised many times to improve its accuracy [9,

[10]. Recently, other than ruby, applications as pressure gauges are beginning to be investigated in various compounds doped with Cr^{3+}, such as $Li_2Mg_3TiO_6$ and MgO[11, 12].

Cr^{3+} stabilizes to the corundum structure (Cr_2O_3:eskolaite) at ambient pressure. Considering the ionic radii, however, in the six-coordination case, doping Cr^{3+} (0.615 Å) adopts a size closer to that of Ga^{3+} (0.620 Å) than Al^{3+} (0.535 Å) [13]. This indicates that Cr^{3+} can more readily displace Ga^{3+} than Al^{3+}. Therefore, doping of Cr^{3+} into corundum-type Ga_2O_3 is thought to be able to impart a function as a fluorescent material as well as in ruby. The β Ga_2O_3 phase, which has a mixed CN of 4 and 6, has been studied with doping of Cr^{3+} [14-16]. Some of these studies have suggested applications to the pressure scale, but reveal that they are limited to use at low temperatures of ca. 85 K[17]. This is probably because of the difference in CN. Recently, there have been studies on the fluorescence properties of Cr-doped corundum-type Ga_2O_3 synthesized from hydroxide GaO(OH) as a precursor[18] and, very recently, on the structural phase transition of Cr-doped β-Ga_2O_3 under metastable room temperature by applying excessive pressure[19]. However, there has been no study on the pressure effects on the R_1 and R_2 lines of single-crystal Cr-doped corundum-type Ga_2O_3 synthesized under high pressure and high temperature conditions. Therefore, in this study, we synthesized high-quality single crystals of Cr-doped corundum-type Ga_2O_3 under high pressure and high temperature, and clarified their fluorescence properties, focusing on the details of the pressure dependence of R_1 and R_2 fluorescence lines, and applied them to the pressure scale.

Experimental

Corundum-type $Ga_2O_3:Cr^{3+}$ was synthesized by a solid-phase reaction method under high temperature and high pressure by using a belt-type apparatus (NIMS: FB30H). As starting samples, Cr_2O_3 (Sigma–Aldrich 99.99% purity) was mixed with ca. 0.1% to 5.0 mol% Ga_2O_3 (Kojyundo Chemical Lab. 99.99% purity), ground in a mortar, and dried under vacuum in an electric furnace at 130°C for 12 h. The sample (enclosed in a gold capsule) was put into a high-pressure cell (Fig. 1). The samples were heated at 1200°C and 7.7 GPa for 1 h to synthesize $Ga_2O_3:Cr^{3+}$ crystals. After rapid quenching by terminating the heater current, the samples were recovered at ambient pressure. The pressure in the sample chamber was calibrated as a function of the press load based on changes in electric resistance associated with a phase transition point of Bi (III-V, 7.7 GPa), Tl (II-III, 3.7 GPa) and Ba (I-II, 5.5 GPa) at room temperature. The temperature of the sample was estimated from the predetermined relationship between the power input and the temperature of the thermocouple (W5%Re – W26%Re) without correction for the pressure effect on the emf.

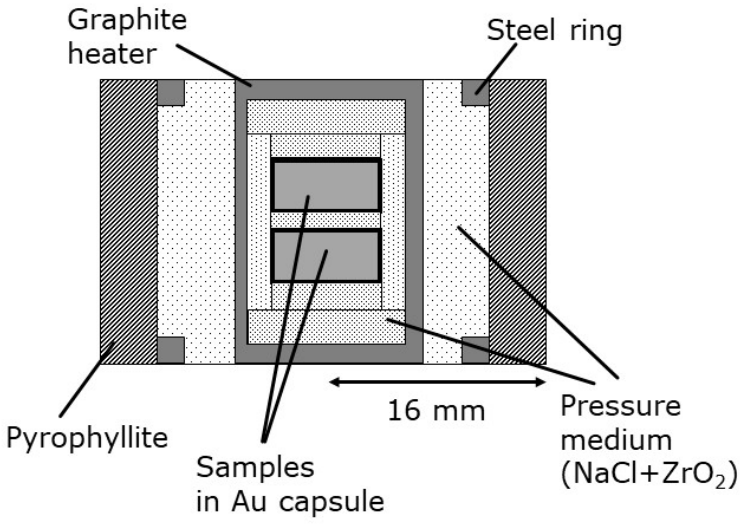

Figure 1. Schematic illustration of the high-pressure cell assembly for synthesizing corundum-type $Ga_2O_3:Cr^{3+}$ crystals.

Structural characterization of the samples by X-ray diffraction (XRD) was performed at synchrotron radiation facilities (AichiSR). Monochromatic X-rays (0.723315 Å), radiated from the superconducting bending magnet at BL2S1, were collimated to a diameter of 100 μm and irradiated the sample fixed on a capillary. The diffracted X-rays, detected with a hybrid pixel array detector (PILATUS 1M, DECTRIS, Switzerland), were converted into intensity–2θ data with IPAnalyzer software[20]. XRD profiles were analyzed by the Rietveld method with GSAS[21]. The quantity of Cr doping in the synthesized crystals was analyzed with an electron probe microanalyzer (EPMA, JXA-8900R, JOEL, Japan). Excitation spectra were measured with a fluorescence spectrometer (FP-8500, JASCO, Japan). The scanning bandwidth of the excitation spectra was 5 nm. High-resolution measurements of R_1 and R_2 fluorescence spectra were made with a 500-mm focal length spectrometer (Andor SR-500i, USA) equipped with a grating (1800 grooves/mm) in combination with a charge-coupled device detector (Andor DU401A, USA). A light-emitting diode (LED) laser with a wavelength of 476.2 nm (LASOS, USA) and focused at 3 μmφ was used as the excitation source. The pressure dependence was determined by measuring R_1 and R_2 spectra from samples placed in a DAC (Syntek, Japan). A single-crystal sample of approximately 20 μm was placed together with a ruby chip into a hole in a stainless-steel gasket of 0.25-mm thickness. A diamond anvil with a culet size of 600 μmφ was used. An alcohol mixed-pressure medium (methanol:ethanol:water = 16:3:1 by volume ratio) was used to maintain hydrostatic pressure in the sample chamber. Ultraviolet (UV) LED light sources of 280 nm (Daico UV-SPOT, Japan) and 365 nm (Keyence UV-300, Japan) were prepared as illumination sources for image observation of the samples under an optical microscope. Detailed observations of the samples at high magnification were made with a laser microscope (Keyence, VK-X1000).

Results and discussion

The recovered $Ga_2O_3:Cr^{3+}$ sample (Cr-doped 1 mol%) was green under LED white light illumination (Fig. 2a), indicating loose sintering. Strikingly, UV illumination changed the color of the sample to deep red (Fig. 2b). The sintered sample consisted of single-crystal aggregates of 20–100 μm in size with well-defined facets (Fig. 2c, d). XRD analysis indicates that the sample was a single phase with a corundum structure. The lattice constants refined by Rietveld analysis are a = 4.9817(1) Å, and c = 13.4362(1) Å (Figure S1). Samples synthesized at other chromium concentrations were also a single phase of corundum. Fig. 3 shows a comparison of the fluorescence images of crystals synthesized at various chromium concentrations. Under the white LED, the intensity of the green color increased with increasing chromium concentration (Fig. 3a). However, under UV illumination, the crystals exhibited different colors as emissions: at a wavelength of 280 nm, the crystals formed at 0.24% Cr concentration were stronger (Fig. 3b); and at a wavelength of 365 nm, 1.0% was the most intense (Fig. 3c). In both cases, a weaker luminescence intensity was observed for the synthesized sample at 4.2% Cr concentration. This is thought to be an effect of concentration quenching, which is common in fluorescent materials.

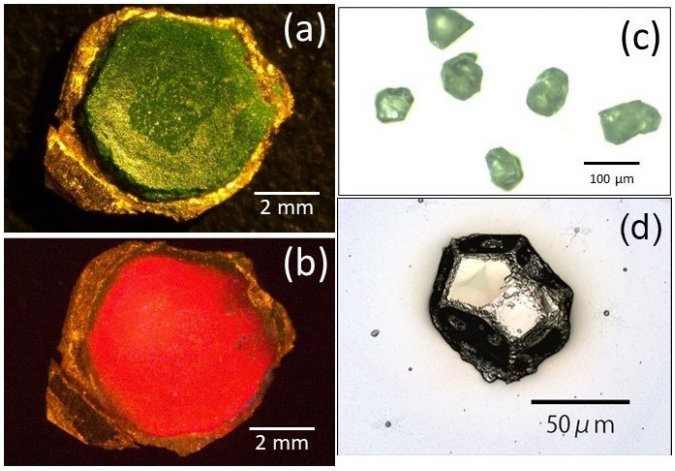

Figure 2. Photographs of high-pressure synthesis of a sintered product (Cr-doped 1 mol %). Images under white LED (a) and UV (b) illumination. Micrographs of single crystals obtained by pulverizing the sintered product and imaging under a microscope (c) and a high-resolution laser microscope (d).

Table 1. Mixing molar ratio of Cr_2O_3 and Ga_2O_3 for starting samples for high-pressure synthesis, and analytical values of Cr concentration (mol %) of products.

Product #	Mixing molar ratio (Cr_2O_3 : Ga_2O_3)	Cr concentration (mol %) EPMA analysis*
1	0.1 : 99.9	0.06(1)
2	0.2 : 99.8	0.24(3)
3	1 : 99	1.0(3)
4	5 : 95	4.2(9)

*Parentheses indicate errors in the last digit.

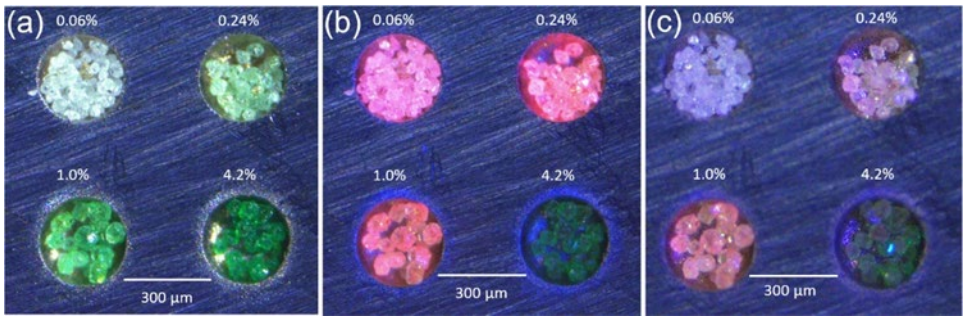

Figure 3. Comparison of the fluorescence images of crystals synthesized at various chromium concentrations: (a) under white LED, (b) with UV (280 nm), or (c) UV (365 nm) light. Crystals were placed into a pit (300 μm in diameter) drilled on stainless-steel plates.

To examine the durability of the temperature change, samples (Cr-doped 1.0 mol%) were placed in an electric furnace and held at each temperature for 1 h; then the samples were removed and analyzed by XRD (Fig. 4) at room temperature. The corundum phase began to change to the β phase at ca. 600°C, and at 800°C it completely changed to the β phase. This demonstrates the high temperature stability as a fluorescent material at ca. 500°C for a high-pressure phase.

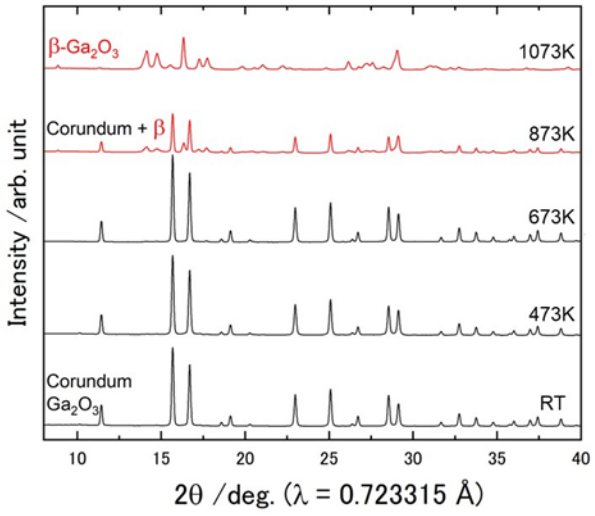

Figure 4. XRD profiles of the products after heat-treatment at each temperature indicated in the figure for 1 h.

Fig. 5 shows excitation spectra (λ_{em} = 697.5 nm) of $Ga_2O_3:Cr^{3+}$ (Cr-doped 1.0 mol%) measured with a fluorescence spectrophotometer, in which the excitation spectrum (λ_{em} = 694.2 nm) of ruby (Cr-doped 1.2 mol%) is also included for comparison. Two large absorption bands were observed in the excitation spectrum. Considering the similarity to the excited states of Cr^{3+} in ruby[22], those absorption bands can be explained by U and Y bands; corresponding to the electron transitions $t^3_{2g}\,{}^4A_{2g} \rightarrow t^2_{2g}e_g\,{}^4T_{2g}$ and $t^3_{2g}\,{}^4A_{2g} \rightarrow t^2_{2g}e_g\,{}^4T_{1g}$, respectively. Regarding ruby, these absorption bands are responsible for the red or pink color of ruby crystals. It is noteworthy that the absorption bands in $Ga_2O_3:Cr^{3+}$ are shifted by 55 nm to the long wavelength side compared with ruby, because of the difference in crystal fields between Al_2O_3 and Ga_2O_3. The shifted absorption bands contribute to $Ga_2O_3:Cr^{3+}$ exhibiting a green color. The combination of U- and Y-band absorption as well as phonon-assisted relaxation leads to the population of the excited $t^3_{2g}\,{}^2E_g$ low-

spin state. This is related to the R lines in the emission spectrum (λ_{ex} = 476.2 nm; Fig. 6), measured with a high-resolution polychrometer. The trigonal field in combination with spin–orbit interaction results in additional splitting, corresponding to R_1 and R_2 lines. Compared with ruby (Fig. 6), the R lines of $Ga_2O_3:Cr^{3+}$ are also shifted to the longer-wavelength side. The fluorescence intensity of the corundum-type $Ga_2O_3:Cr^{3+}$ has a clearly higher intensity than ruby (Figure S2).

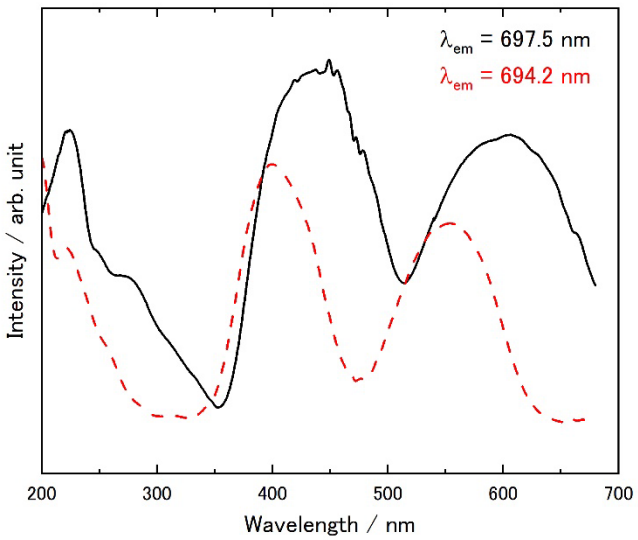

Figure 5. Excitation spectrum (λ_{em} = 697.5 nm) of $Ga_2O_3:Cr^{3+}$ (Cr-doped 1.0 mol%) (solid line). Excitation spectrum (λ_{em} = 694.2 nm) of ruby (Cr-doped 1.2 mol%) is also included for comparison (dashed line).

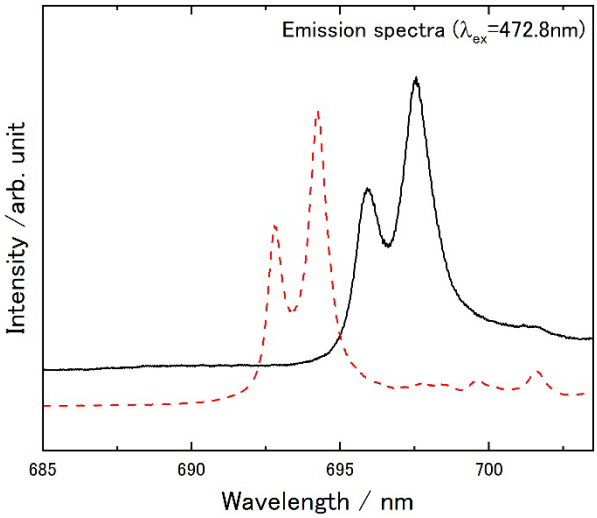

Figure 6. Emission spectrum (λ_{ex} = 472.8 nm) of $Ga_2O_3:Cr^{3+}$ (Cr-doped 1.0 mol%) (solid line). Excitation spectrum (λ_{ex} = 472.8 nm) of ruby (Cr-doped 1.2 mol%) is also included for comparison (dashed line).

In the present $Ga_2O_3:Cr^{3+}$, the R_1 and R_2 lines are also applicable as a pressure scale as well as ruby. Therefore, their pressure-dependence was measured by comparing them to ruby in the hydrostatic pressure range. Each peak position was determined by multiple curve fitting with a pseudo-Voigt function. Fig. 7 shows the pressure dependence of the R_1 peak in $Ga_2O_3:Cr^{3+}$, in which the pressure was determined in correspondence with the ruby pressure scale for R_1 peaks in accordance with Mao et al. (1986)[9]. The equations for pressure scale obtained by linear regression for all R_1 or R_2 data is as follows,

$$P_{R1} = (\lambda - \lambda_0) / 0.314, \qquad [1]$$

$$P_{R2} = (\lambda - \lambda_0) / 0.326, \qquad [2]$$

where P indicates pressure (GPa); and λ_0 and λ denote the wavelength (nm) of these peaks at ambient pressure and at any pressure, respectively. For an easy comparison, linear regression of the R_1 and R_2 data in ruby gives the following equations,

$$P_{R1} = (\lambda - \lambda_0) / 0.358, \qquad [3]$$

$$P_{R2} = (\lambda - \lambda_0) / 0.365. \qquad [4]$$

Compared with ruby, $Ga_2O_3:Cr^{3+}$ has somewhat less pressure-dependence (Fig. 7) but it is still acceptable as a pressure scale.

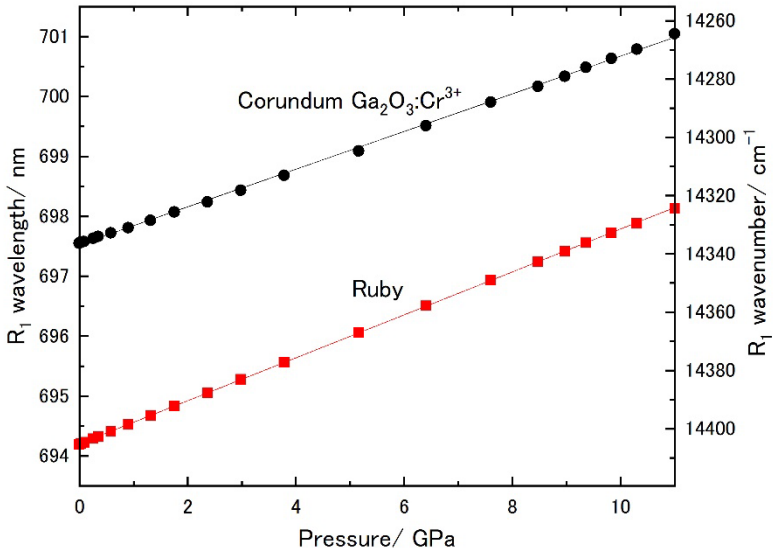

Figure 7. Pressure dependence of R_1 and R_2 peaks of $Ga_2O_3:Cr^{3+}$ (circles) and ruby (squares). Straight lines are the regression line determined by the least-squares method.

Because the R_1 and R_2 peaks overlap, it is pertinent in terms of the practicality of the pressure scale to consider the degree of separation of the peaks. Fig. 8 shows the pressure variation of the peak shape along with an example of fitting by the peak function. For detailed discussion of peak separation, not only must the difference between the respective peak positions be considered but also the full width at half maximum (FWHM) of each peak. Fig. 9(a) shows the difference in peak positions of R_1 and R_2 for $Ga_2O_3:Cr^{3+}$ and ruby, respectively. The FWHMs of R_1 and R_2 are plotted in Fig. 9(b) and 9(c) for $Ga_2O_3:Cr^{3+}$ and ruby, respectively. In terms of the difference in peak positions, $Ga_2O_3:Cr^{3+}$ was better-separated than ruby at all pressures. Regarding the FWHM, the values at each of the ruby peaks were nearly constant or slightly increasing with increasing pressure. However, the FWHM of $Ga_2O_3:Cr^{3+}$ substantially decreased with increasing pressure.

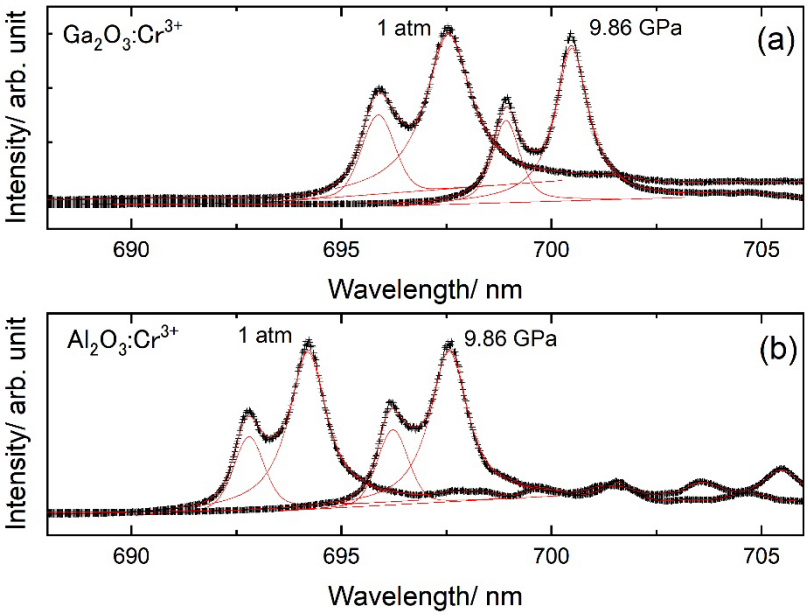

Figure 8. Pressure variation of the peak shape along with an example of fitting by a pseudo-Voigt function. Spectra at ambient pressure and 9.86 GPa of $Ga_2O_3:Cr^3$ (a) and ruby (b).

By applying a commonly used index (resolution, R_s) in chromatography, the degree of peak separation between $Ga_2O_3:Cr^{3+}$ and ruby was compared. Resolution R_s is one indicator of peak separation by both the peak position difference and FWHM. The R_s is defined by a following equation,

$$R_s = (\lambda_{R1} - \lambda_{R2}) / (1/2) \cdot (W_{R1} + W_{R2}), \qquad [5]$$

where λ and W denote the wavelength (nm) and peak width, respectively. Assuming a Gaussian peak shape, the equation can be rewritten by using the FWHM (Wh) as follows,

$$R_s = 1.18 \times (\lambda_{R1} - \lambda_{R2}) / (Wh_{R1} + Wh_{R2}). \qquad [6]$$

Because the present pseudo-Voigt function is not Gaussian, the coefficient of 1.18 should be different. However, for relative comparisons it is acceptable to consider the coefficient as unity.

Fig. 10 shows the R_s for $Ga_2O_3:Cr^{3+}$ and ruby. Here, higher R_s values indicate that the peaks are well-separated. Strikingly, contrary to ruby, the R_s of $Ga_2O_3:Cr^{3+}$ increased with increasing pressure. Therefore, the pressure scale with $Ga_2O_3:Cr^{3+}$ is considered to have an advantage over ruby in terms of measurement accuracy up to ca. 35 GPa, where the phase transition to Rh_2O_3(II) may occur[3, 4]. In Ga_2O_3, given that the corundum structure is a stable phase under high pressure, it is a metastable phase with a relaxed structure under ambient pressure. There, Cr is considered to exist in the 6-coordination site of the metastable state structure. The separation of the R_1 and R_2 lines tends to be affected by the structural relaxation, and thus the degree of separation is considered to be poor at ambient pressure. Conversely, as the pressure increases, the structure becomes more stabilized as it reaches the stable region of the corundum structure. Accordingly, the separation of the peaks is considered to be better.

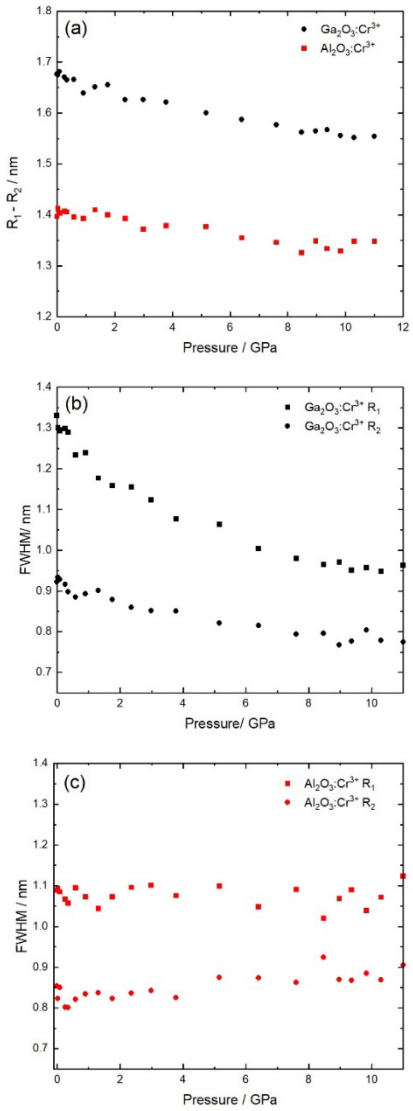

Figure 9. (a) Difference in peak positions of R_1 and R_2 for $Ga_2O_3:Cr^{3+}$ (circles) and ruby (squares), respectively. (b) FWHM of the R_1 (circles) and R_2 (squares) peaks of $Ga_2O_3:Cr^{3+}$. (c) FWHM of the R_1 (circles) and R_2 (squares) peaks of $Al_2O_3:Cr^{3+}$.

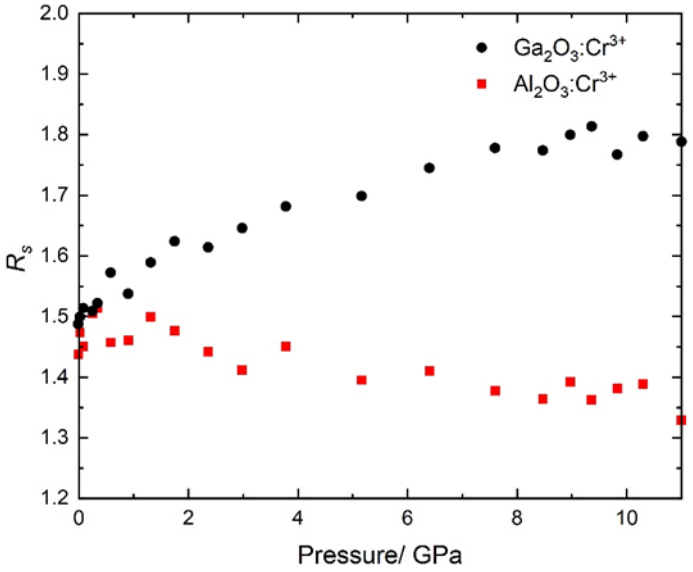

Figure 10. Change of resolution (R_s) between R_1 and R_2 peaks of $Ga_2O_3:Cr^{3+}$ (circles) and $Al_2O_3:Cr^{3+}$ (squares) with increasing pressure.

With respect to the excitation spectra that excite R_1 and R_2 fluorescence, $Ga_2O_3:Cr^{3+}$ is substantially shifted to the longer wavelength than ruby, as described in a previous paragraph. Furthermore, it is assumed that the excitation spectrum is also pressure-dependent. Regarding of the ruby excitation spectrum, its pressure dependence has been previously measured by Duclos (1990), indicating that both the U and Y bands shift toward the lower wavelength side by approximately 50 nm with a pressure change of 30 GPa. Now consider the laser source that excites the pressure markers in the DAC. The previously used 488-nm (Ar-ion) laser excites $Ga_2O_3:Cr^{3+}$ well at the low-pressure range. Furthermore, the 532-nm (YAG second harmonic) lasers that are commonly used efficiently excite $Ga_2O_3:Cr^{3+}$ to higher-pressure regions compared with ruby. Moreover, even He–Ne (632 nm), emitting red light, could be available to excite corundum-type

$Ga_2O_3:Cr^{3+}$ crystals as indicated in Figure S3. This indicates that the $Ga_2O_3:Cr^{3+}$ is more versatile than ruby.

SUMMARY

We succeeded in doping Cr^{3+} into Ga_2O_3 with a corundum structure by high-temperature and high-pressure synthesis. The crystals show green color under white illumination and red fluorescence under UV light irradiation. The pressure dependence of the R_1 and R_2 peaks in the fluorescence spectra is available on the pressure scale for DAC as well as ruby fluorescence. The R_1 and R_2 peaks were well separated with increasing pressure. As compared to ruby, the excitation spectrum is shifted to the longer wavelength. This indicates that excitation with lasers of longer wavelengths is possible. Therefore, the $Ga_2O_3:Cr^{3+}$ is more versatile than ruby with respect to application to the pressure scale.

AUTHOR INFORMATION

Corresponding Author

Hitoshi Yusa – High-Pressure Structural Control Group, Research Center for Materials Nanoarchitechtonics, National Institute for Materials Science, 1-1 Namiki (NIMS), Tsukuba, Ibaraki 305-0044, Japan. Email: yusa.hitoshi@nims.go.jp

Author

Masashi Miyakawa – High-Pressure Structural Control Group, Research Center for Materials Nanoarchitechtonics, National Institute for Materials Science, 1-1 Namiki (NIMS), Tsukuba, Ibaraki 305-0044, Japan.

Author Contributions

The manuscript was written through contributions of all authors. All authors have given approval to the final version of the manuscript.

Notes

The authors declare no competing financial interest.

ACKNOWLEDGMENT

The synchrotron radiation experiments were conducted at BL2S1 in AichiSR and BL18C in Photon Factory (KEK), and BL2S1 in AichiSR with the approval of AichiSR (Proposal No. 2023N1003, 2023N3003), and KEK (Proposal No. 23G570), respectively. This work was supported by JSPS KAKENHI (Grant Nos. 19H05790, and 23K17711). We are grateful to Y. Umena, H. Onoda, and Y. Shibazaki for their help with the X-ray diffraction experiments at the synchrotron facilities. We also thank M. Nishio for their assistance with EPMA analyses. This work was supported by World Premier International Research Center Initiative (WPI).

REFERENCES

(1) Higashiwaki, M.; Sasaki, K.; Kuramata, A.; Masui, T.; Yamakoshi, S. Development of gallium oxide power devices. *physica status solidi (a)* **2014**, *211* (1), 21-26.
(2) Pearton, S. J.; Yang, J.; Cary, P. H., IV; Ren, F.; Kim, J.; Tadjer, M. J.; Mastro, M. A. A review of Ga_2O_3 materials, processing, and devices. *Applied Physics Reviews* **2018**, *5* (1), 011301.
(3) Yusa, H.; Tsuchiya, T.; Sata, N.; Ohishi, Y. Rh_2O_3(II)-type structures in Ga_2O_3 and In_2O_3 under high pressure: Experiment and theory. *Phys. Rev. B* **2008**, *77* (6), 064107.
(4) Tsuchiya, T.; Yusa, H.; Tsuchiya, J. Post-Rh_2O_3(II) transition and the high pressure-temperature phase diagram of gallia: A first-principles and x-ray diffraction study. *Phys. Rev. B* **2007**, *76* (17), 174108.
(5) Remeika, J. P.; Marezio, M. Growth of alpha-Ga_2O_3 single crystals at 44 kbars *Appl. Phys. Lett.* **1966**, *8* (4), 87-88.
(6) Prewitt, C. T.; Shannon, R. D.; Rogers, D. B.; Sleight, A. W. C rare earth oxide-corundum transition and crystal chemistry of oxides having corundum structure. *Inorg. Chem.* **1969**, *8* (9), 1985-1993.
(7) Syassen, K. Ruby under pressure. *High Pressure Research* **2008**, *28* (2), 75-126.
(8) Piermarini, G. J.; Block, S.; Barnett, J. D.; Forman, R. A. Calibration of pressure-dependence of R1 ruby fluorescence line to 195 kbar. *J. Appl. Phys.* **1975**, *46* (6), 2774-2780.

(9) Mao, H. K.; Xu, J.; Bell, P. M. Calibration of the ruby pressure gauge to 800-kbar under quasi-hydrostatic conditions. *Journal of Geophysical Research-Solid Earth and Planets* **1986**, *91* (B5), 4673-4676.
(10) Zha, C.-S.; Mao, H.-k.; Hemley, R. J. Elasticity of MgO and a primary pressure scale to 55 GPa. *Proceedings of the National Academy of Sciences* **2000**, *97* (25), 13494-13499.
(11) Szymczak, M.; Woźny, P.; Runowski, M.; Pieprz, M.; Lavín, V.; Marciniak, L. Temperature invariant ratiometric luminescence manometer based on Cr3+ ions emission. *Chem. Eng. J.* **2023**, *453*.
(12) Szymczak, M.; Runowski, M.; Lavín, V.; Marciniak, L. Highly Pressure ‐ Sensitive, Temperature Independent Luminescence Ratiometric Manometer Based on MgO:Cr3+ Nanoparticles. *Laser & Photonics Reviews* **2023**, *17* (4).
(13) Shannon, R. D. Revised effective ionic-radii and systematic studies of interatomic distances in halides and chalcogenides. *Acta Crystallographica Section A* **1976**, *32* (SEP1), 751-767.
(14) Walsh, C. G.; Donegan, J. F.; Glynn, T. J.; Morgan, G. P.; Imbusch, G. F.; Remeika, J. P. Luminescence from β-Ga_2O_3:Cr^{3+}. *J. Lumin.* **1988**, *40-41*, 103-104.
(15) Luchechko, A.; Vasyltsiv, V.; Zhydachevskyy, Y.; Kushlyk, M.; Ubizskii, S.; Suchocki, A. Luminescence spectroscopy of Cr^{3+} ions in bulk single crystalline β-Ga_2O_3. *J. Phys. D: Appl. Phys.* **2020**, *53* (35), 354001.
(16) Chen, K.-C.; Fang, M.-H.; Huang, W.-T.; Kamiński, M.; Majewska, N.; Leśniewski, T.; Mahlik, S.; Leniec, G.; Kaczmarek, S. M.; Yang, C.-W.; et al. Chemical and Mechanical Pressure-Induced Photoluminescence Tuning via Structural Evolution and Hydrostatic Pressure. *Chem. Mater.* **2021**, *33* (10), 3832-3840.
(17) Beales, T. P.; Goodman, C. H. L.; Scarrott, K. A new high-pressure calibrant: β-Ga_2O_3:Cr. *Solid State Commun.* **1990**, *73* (1), 1-3.
(18) Back, M.; Ueda, J.; Nambu, H.; Fujita, M.; Yamamoto, A.; Yoshida, H.; Tanaka, H.; Brik, M. G.; Tanabe, S. Boltzmann Thermometry in Cr3+-Doped Ga2O3 Polymorphs: The Structure Matters! *Advanced Optical Materials* **2021**, *9* (9), 2100033.
(19) Majewska, N.; Muñoz, A.; Liu, R.-S.; Mahlik, S. Influence of Chemical and Mechanical Pressure on the Luminescence Properties of Near-Infrared Phosphors. *Chem. Mater.* **2023**, *35* (12), 4680-4690.
(20) Seto, Y.; Nishio-Hamane, D.; Nagai, T.; Sata, N. Development of a software suite on X-ray diffraction experiments. *Review of High Pressure Science and Technology* **2010**, *20* (3), 269-276.
(21) Larson, A. C.; Von Dreele, R. B. General structure analysis system (GSAS). *Los Alamos National Laboratory Report LAUR* **2004**, 86-748.
(22) Kushida, T. Absorption Spectrum of Optically Pumped Ruby I. Experimental Studies of Spectrum in Excited States. *J. Phys. Soc. Jpn.* **1966**, *21* (7), 1331-1341.

SYNOPSIS

Cr^{3+}-doped Ga_2O_3 crystals with a corundum structure were synthesized under high temperature and high pressure. The crystals were green under white light illumination but deep red when exposed to ultraviolet light. The pressure dependence of the R_1 and R_2 peaks in the

fluorescence spectra is available on the pressure scale for DAC as well as ruby fluorescence. The excitation spectrum was shifted to the long-wavelength side compared with ruby, which enables excitation with long-wavelength lasers, even if the pressure effect is considered. In addition, the R_1 and R_2 peaks were well-separated with increasing pressure, which might have advantages over the ruby scale.